Comparison of SPAD Readings and Satellite Spectral Reflectance to Assess the Health Status of Declining *Ficus microcarpa* Street Trees

JAMES KOMEN, CAMILLE C. PAWLAK, AND DONALD R. HODEL

Abstract

Healthy urban forests provide a suite of ecosystem services and amenities to cities and residents. Urban forest health can be monitored through field techniques, such as SPAD meter chlorophyll measurements, spectral reflectance values from satellite imagery, and imagery from Google Maps Street View. Satellite imagery and Google Maps Street View (GMSV) allow access to historical and relatively recent conditions. This paper evaluates all three of these sources for detecting decline in a set of *Ficus microcarpa* street trees in Lakewood, California, U. S. A. A planting of 25 *Ficus microcarpa* street trees was assessed in three phases: field observations and SPAD measurement; subjective health and canopy density ratings based on historical Google Maps Street View images; and spectral reflectance values in four bands from Worldview-II satellite data collected in 2010, 2012, 2016, and 2018. Data from each of 28 input variables were analyzed for correlation. Generally, five categories of strong variable pair relationships existed: (1) Field/GMSV Relationship, (2) GMSV/Satellite Relationship, (3) Consistency Over Time, (4) Observation Self-Consistency, and (5) Satellite Self-Consistency. The strongest correlations were between adjacent bands of reflectance collected in the same year ($|r| \sim 1$ to 0.85) and between subjectively rated health and canopy density ratings ($r \sim 0.91$ to 0.82). There was a significant difference in the Near-Infrared reflectance values between the trees with and without a history of recent root pruning ($p < 0.06$ and $p < 0.05$).

Key Words: Indian Laurel Fig, Remote Sensing, Tree Survey Techniques

Introduction

Healthy urban forests can provide a suite of ecosystem services and amenities to cities and residents, which, when well-managed, can be measured and reported. Pushes in green

infrastructure in the last 60 years have led to thoughtful management that measures and calculates these services and amenities (Carreiro et al. 2007). Street trees represent a publicly managed portion of the urban forest and green infrastructure. In California, where 95% of residents live in urbanized areas, an estimated 9.1 million street trees are present (US Census Bureau Public Information Office 2010; McPherson et al. 2016). These trees provide essential amenities and benefits to urban residents by aiding in climate control, providing energy-savings, reducing impervious runoff and water quality, creating complex urban habitat for biodiversity, reducing particulate pollution, and sequestering carbon (Livesley et al. 2016). The extent of the benefits provided by urban trees to cities depends on the health of the trees and the urban forest diversity and structure (Livesley et al. 2016).

The structure, health, and diversity of urban forests are frequently recorded through municipal tree inventories (Cumming et al. 2008). Traditional tree inventories are completed by field technicians traveling from tree to tree and recording tree characteristics. This activity requires a significant physical effort and takes considerable time to document every street tree in an urban forest. These inventories can only be updated as the budget and temporal restraints allow. Such restraints on inventory updates can make it difficult to identify quickly when a tree's health is in decline or when maintenance might be appropriate to maximize the ecosystem amenities and benefits a tree provides.

Recently, remote sensing tools such as satellite imagery have been used more frequently to monitor tree traits, like health, in urban forest inventories (Morgenroth and Östberg 2017; Fang et al. 2020). Traditionally, tree health has been recorded in inventories through different techniques such as visual observations by field technicians, SPAD meter readings, and remote sensing techniques. Vegetation has unique spectral characteristics that can be identified using remote sensing (Xie et al. 2008). In particular, the Red, Red-Edge and Near-Infrared regions of the electromagnetic spectrum have relevance for vegetation mapping (Xie et al. 2008). Vegetation has high reflectance in the Near-Infrared region due to internal leaf scattering and absorption (Knipling 1970). In the Red visible spectrum, chlorophyll absorption results in a low vegetation reflectance (Xie et al. 2018). The Red-Edge spectrum can be used to detect stress in vegetation by assessing chlorophyll status and leaf area index independent of ground cover conditions (Horler et al. 1983). Using satellite data, normalized difference vegetation indices (NDVI) have been employed as a proxy for tree health using the red and Near-Infrared bands (Malthus et al. 2000). Measurements from field tools like the SPAD meter, which is used to measure chlorophyll content, have been correlated to satellite measurements of NDVI (Robson et al. 2014). Literature has been published that uses Google Maps Street View (GMSV) to record urban forest canopy cover and compares SPAD measurement to satellite-sensed vegetation indices for crops and satellite-sensed NDVI to street tree health, but no literature has assessed

how field-based tree health measurements, GMSV-based tree health measurements, individual satellite band values, and SPAD meter measurements are correlated for urban street trees (Wu et al. 2007; Wu et al. 2019; Xia et al. 2021; Richards and Edwards 2021). Our research assesses correlations between field measurements, satellite measurements, and GSMV measurements for health status of an urban street tree *Ficus microcarpa* (Chinese banyan, Indian laurel fig) in Lakewood, California, U. S. A., and suggests which techniques cities can be meaningfully used to maintain up-to-date tree health assessments for street tree inventories.

Materials and Methods

In May of 2018, we selected 51 *Ficus microcarpa* trees growing along the 4200 to 4700 block of Paramount Blvd. in Lakewood, California, U. S. A. (**Fig. 1**). All selected trees were approximately the same age and spacing along the street growing in 4-meter-wide irrigated median strips with regularly maintained turfgrass cover. We chose these trees because they were on a busy urban road that appeared in multiple years of Google Maps Street View imagery and were uniformly planted in an easily and publicly accessible area.

Trees 1 through 44 were on the eastern side of the street and exhibited varying degrees of decline symptoms in 2018. Dead branches had not been pruned off for six years; thus, this sample set was useful for collecting data on their history of decline over an extended period. The trees ranged in size from 31 to 95 centimeters diameter at standard height (DSH), with an average of 59 centimeters. They ranged in height from 6 to 12 meters with an average of 8 meters. The trees had a history of root pruning from between 2013 and 2015 to mitigate curb damage. Root cuts were between 2 and 3 meters from the trunks and along the eastern side of the root system.

For comparison with the data collected from Trees 1 through 44, we selected a second set of nearby *Ficus microcarpa* on the same street. This second set of trees were the same age and appeared to be healthy. Trees 45 through 51 were along the western side of Paramount Blvd., just south of Trees 1 through 44. They had broader, denser canopies and ranged in size from 56 to 98 centimeters DBH with an average of 72 cm. They ranged in height from 9 to 15 meters with an average of 13 meters. Although evidence of past surface root damage from lawn mowing was visible, no curb replacement and root pruning had occurred within the past few years.

All 51 trees in the study had a history of stress when statewide drought restrictions were implemented in 2015. Sprinkler irrigation along the median strips was reduced and then completely shut off, causing much of the turfgrass in the median strips to die. The combination of drought stress and past root pruning on Trees 1 through 44 likely led to their declining

Fig. 1. Map of trees featured in this study. Trees are labeled with their identification numbers. Red X's mark trees that were skipped. © Google Earth.

condition. Typically, such stressful conditions leave the tree susceptible to a host of secondary diseases and pests. Although we did not perform pathological assessments of declining trees, a disease called bot canker fungus or *Ficus* branch dieback (*Botryossphaeria*) is often a secondary invader of *Ficus microcarpa* subjected to a history of periodic root pruning and other stresses,

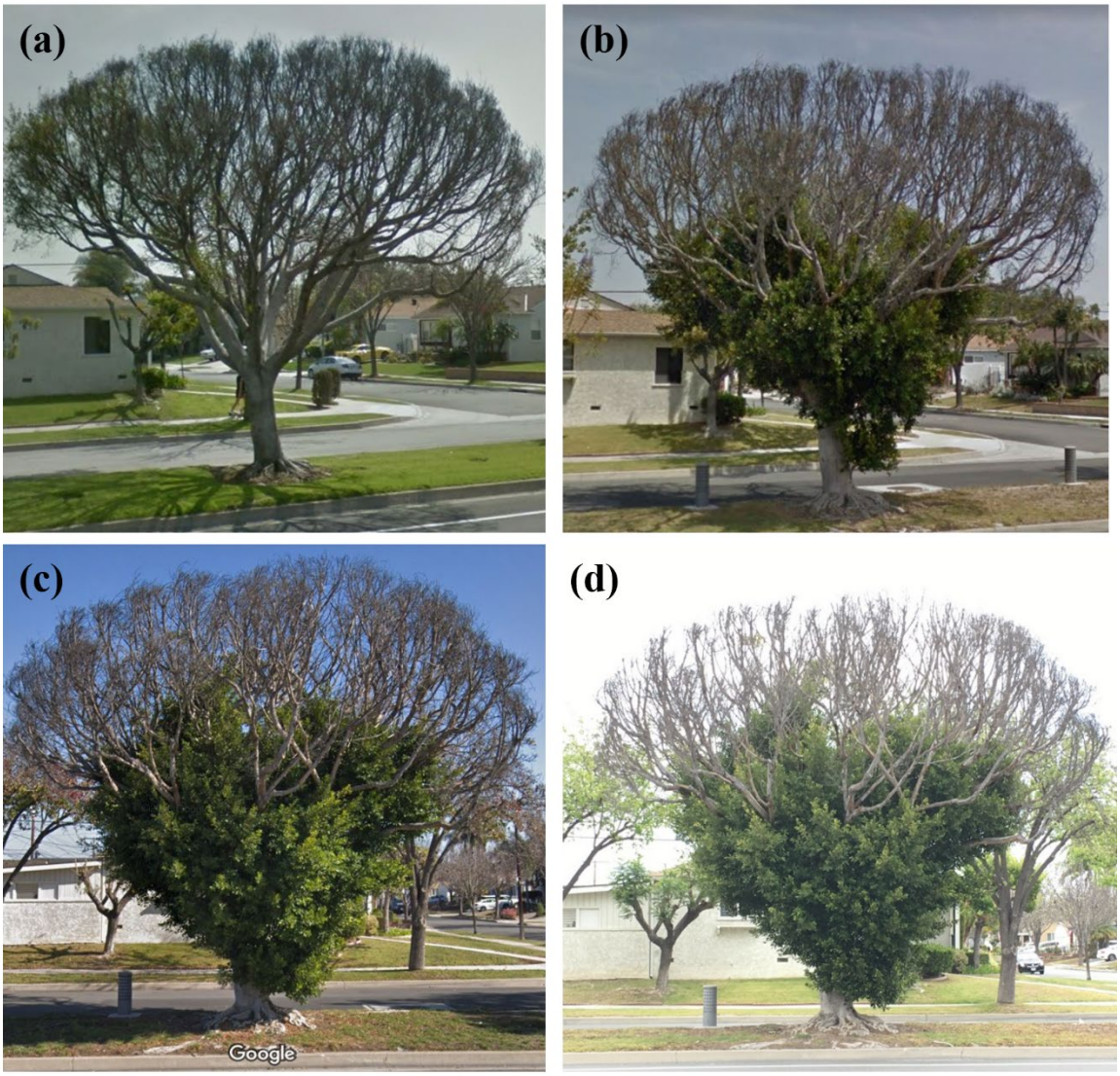

Fig. 2. Comparison of the photos taken of Tree 6, *Ficus microcarpa*, Lakewood, California: a. 2011; b. 2016; c. 2018; d. 2018. a–c © Google Street View, selected closest to the satellite data collection dates; d. © J. Komen, taken at time of field data collection (2018).

and bot canker fungus may have contributed to the trees' decline of health (Hodel et al. 2009; Mayorquin et al. 2012a, 2012b). Bot canker fungus in Indian laurel fig trees leads to branch dieback, crown thinning, and possible tree death (Mayorquin et al. 2012a). In December of 2019, all the trees in this study were removed due to their poor health.

We completed data collection in three phases. In phase 1, on May 14th, 2018, we collected field data. In phase 2, we aggregated historical GMSV imagery of the trees, and authors Komen and Hodel used this imagery to rate the trees' appearances visually. In phase 3 we aggregated

historical Worldview-II satellite data of the trees. Due to limitations in the available satellite imagery, we fully analyzed only 25 of the 51 trees.

In phase 1, we photographed, measured, and visually assessed each of the trees for five attributes: health, growth decline phase, canopy density, root pruning damage, and turfgrass mower damage (**Fig. 2**). We rated tree health subjectively on a scale of 1 to 5 with 1 being *dead* and 5 being *excellent health*. We subjectively assigned a growth decline phase of one of four classifications to each tree: (A) Good condition, not declining; (B) Good condition, but declining; (C) Poor condition, but improving; or (D) Poor condition, not improving. We rated canopy density subjectively rated on a scale of 0 to 100%, where a dense canopy would receive a higher rating. We assessed root pruning and mower damage as binary attributes: if evidence of root pruning or mower damage was observed, it was noted. Authors Komen and Hodel collaboratively agreed upon condition ratings.

We collected SPAD data from the trees by randomly sampling 10 leaves from the upper canopy of each tree because they were directly exposed to satellite measurements. Under authors Komen's and Hodel's direction, an arborist randomly collected these leaves using an aerial lift truck. We took one reading from each leaf and averaged reading for all 10 leaves from each tree. In phase 1, we assessed a total of 47 trees. Trees 20, 21, 25, and 44 were excluded from the phase 1 because they were inaccessible for SPAD data collection during our field survey.

After the field data collection phase, we aggregated historical GMSV images of each of the subject trees. Google Street View imagery was available for December 2008, April 2011, February 2015, April 2016, December 2017, and February 2018. We recorded only the month and year of the street view images because GMSV does not include the day or time of its images. Once the data was collected, we subjectively rated the growth phase, canopy density, and health of each tree at each point in time. Authors Komen and Hodel assessed each of the variables on the same scale as in Phase 1. Images of Trees 8 through 10 were unavailable in street view, so these were excluded from the analysis.

In Phase 3, we extracted reflectance values for our study trees from the Worldview-II Satellite for the Red (630 nm to 690 nm), Red-Edge (700 nm to 745 nm), Near Infrared-1 (770 nm to 895 nm), and Near Infrared-2 (895 nm to 950 nm) bands from the following dates: April 7, 2010, April 28, 2012, May 24, 2016, and April 11, 2018 (**Fig. 3**). Dates were selected to match the GMSV imagery dates as closely as possible. Worldview-II data was normalized from digital number values to surface reflectance using the DigitalGlobe Atmospheric Compensation algorithm to minimize variation in imagery due to illumination, viewing geometry, and atmospheric affects. To obtain

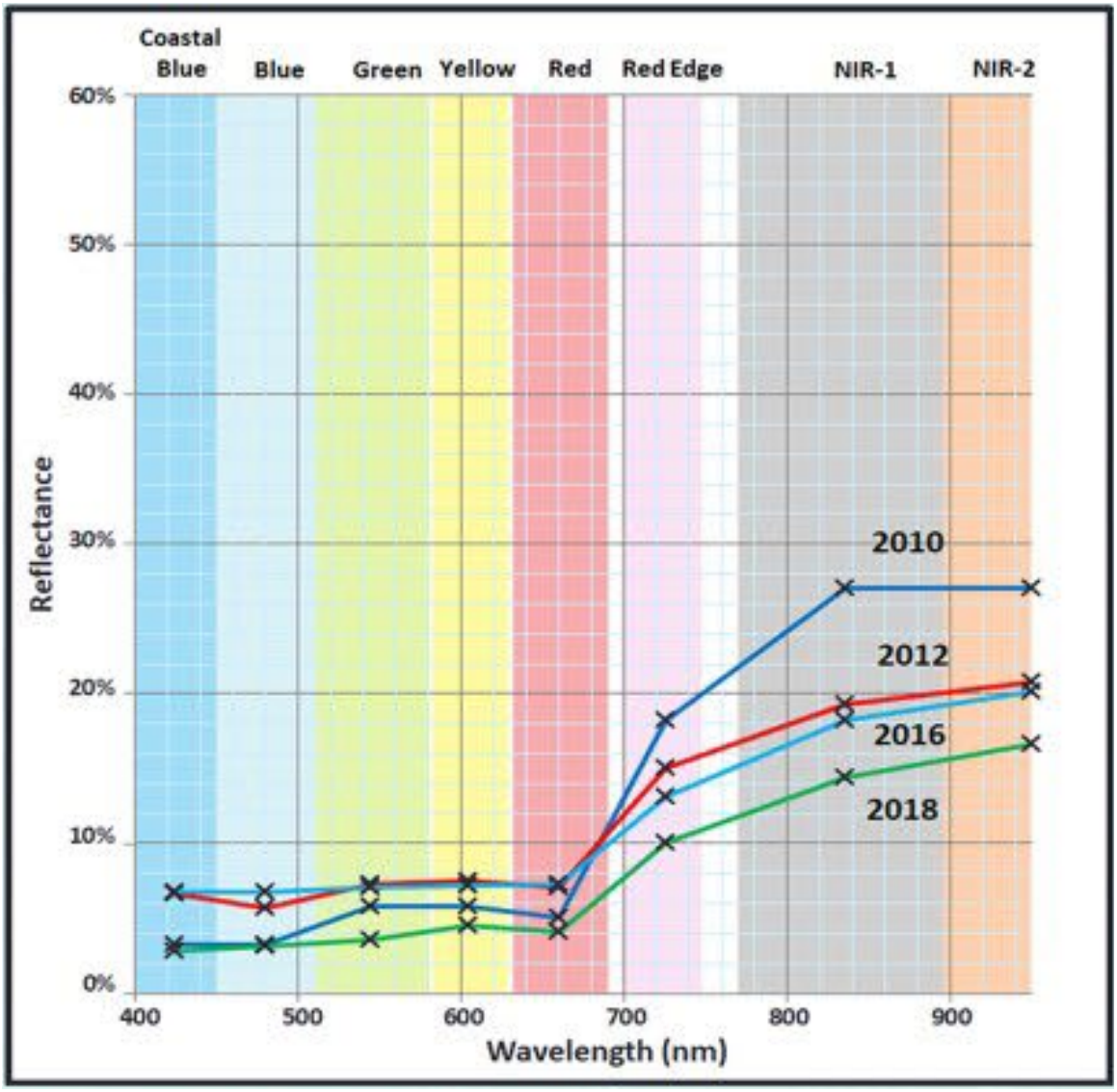

Fig. 3. Satellite reflectance curve for Tree 6, *Ficus microcarpa*, Lakewood, California, showing the different values for each reflectance band at each historical collection interval (2010 to 2018).

an average spectral reflectance percent value for each band for each tree, we averaged the pixel values for ten manually selected pixels that contained pure canopy (avoiding areas in shadow, or mixed pixels from the edge of the canopy) within each tree's canopy spread. We visually determined the span of pixel values for each tree by viewing the Worldview-II Satellite data in the visible light spectrum. Due to thin canopies, some trees' reflectance values were indistinguishable in the satellite imagery, so we omitted reflectance values for these trees fromour analysis. Instead, we limited the results of the satellite data query to 19 trees from the

first set (1 through 3, 6 through 8, 10 through 13, 15, 22, 23, 27 through 29, 31, 36, and 41) and 6 trees from the second set (45, 46, and 48 through 51) (**Fig. 1**).

After the three phases of data collection, we assembled a correlation matrix to show the relationships between each of the recorded variables. We assessed each correlated pair over the set of trees with available data. For example, Worldview-II data was not available for Trees 4 and 5, and GMSV data was not available for Trees 8 through 10, so we excluded these trees in correlation analysis for satellite reflectance and GMSV observations. We ranked correlations of each variable pair from highest to lowest absolute value.

For our historical observations from GMSV and the Worldview-II satellite, we created a correlation matrix of the aggregated data across each of the four periods. For each observation of canopy density and health from GMSV, we calculated correlation coefficients for satellite reflectance for each period.

Results

For each of the 841 permutations in our correlation matrix, we analyzed the correlation coefficients and r^2 values. All variables with a correlation coefficient of above 0.7 are highlighted in this paper, ranging from r ~ 0.7 to 0.99 (**Table 1**). The strength of the correlations is ranked from weak to strong according to the scale for correlation coefficients from Bruce (2009) (correlations where $r \geq 0.7$ are rated as strong). Six of the seven sets of variables with the highest correlation were pairs of satellite data for adjacent bands of reflectance in the same year. Near Infrared-1 had a strong correlation ($r > 0.96$) with Near Infrared-2 in each of the years that satellite data was collected. Health and canopy density ratings were also self-consistent; within the same year, they tended to correlate ($r > 0.88$) with each other, showing that the trends shown in this study are not due to inconsistencies in data collection. Ten of the strong correlations showed consistency over time for the same set of trees.

Field canopy density and field-based health ratings were strongly correlated ($r > 0.88$). Field measurements of canopy density were correlated with both GSMV measurements of canopy density (r ~ 0.82) and health (r ~ 0.82), and field measurements of health were correlated with both GSMV measurements of canopy density (r ~ 0.92) and health (r ~ 0.91). In 2012, Red-Edge reflectance data was strongly negatively correlated with the GMSV condition ratings ($r < -0.76$) In 2010 and 2012, the NIR-1 and NIR-2 bands were correlated with GMSV ratings for health and canopy density ($r > 0.7$). Red band reflectance data from 2018 was negatively correlated with both SPAD measurements (r ~ -0.73) and field-assessed health (r ~ -0.73) from 2018.

Rank	Source 1	Variable 1	Source 2	Variable 2	r	r^2	Relevance
1	Satellite	NIR-1 2016	Satellite	NIR-2 2016	1.00	0.99	Satellite Self-consistency
2	Satellite	NIR-1 2012	Satellite	NIR-2 2012	0.99	0.98	Satellite Self-consistency
3	Satellite	NIR-1 2018	Satellite	NIR-2 2018	0.99	0.98	Satellite Self-consistency
4	Satellite	NIR-1 2010	Satellite	NIR-2 2010	0.96	0.93	Satellite Self-consistency
5	Satellite	Red 2016	Satellite	NIR-2 2016	0.96	0.92	Satellite Self-consistency
6	GMSV	Health 2016	GMSV	Health 2018	0.96	0.91	Consistency over time
7	Satellite	Red 2016	Satellite	NIR-1 2016	0.96	0.91	Satellite Self-consistency
8	GMSV	Canopy Density 2010	GMSV	Health 2010	0.94	0.89	Observation self-consistency
9	GMSV	Canopy Density 2010	GMSV	Health 2012	0.94	0.89	Consistency over time
10	GMSV	Health 2010	GMSV	Canopy Density 2012	0.94	0.89	Consistency over time
11	GMSV	Canopy Density 2012	GMSV	Health 2012	0.94	0.89	Observation self-consistency
12	GMSV	Canopy Density 2016	GMSV	Canopy Density 2018	0.93	0.86	Consistency over time
13	GMSV	Canopy Density 2016	GMSV	Health 2016	0.92	0.85	Observation self-consistency
14	Field	Health 2018	Field	Canopy Density 2018	0.92	0.84	Observation self-consistency
15	Field	Health 2018	GMSV	Health 2018	0.91	0.83	Field/GMSV relationship
16	GMSV	Canopy Density 2016	GMSV	Health 2018	0.89	0.80	Consistency over time
17	GMSV	Canopy Density 2018	GMSV	Health 2018	0.89	0.79	Observation self-consistency
18	Satellite	Red Edge 2012	Satellite	NIR-1 2012	-0.89	0.78	Satellite Self-consistency
19	Field	Health 2018	GMSV	Canopy Density 2018	0.88	0.78	Field/GMSV relationship
20	Satellite	Red Edge 2012	Satellite	NIR-2 2012	-0.88	0.77	Satellite Self-consistency
21	Satellite	Red 2012	Satellite	NIR-1 2012	0.85	0.73	Satellite Self-consistency
22	Satellite	Red 2012	Satellite	NIR-2 2012	0.85	0.72	Satellite Self-consistency
23	GMSV	Canopy Density 2010	Satellite	Red Edge 2012	-0.84	0.71	-
24	Satellite	Red Edge 2012	GMSV	Canopy Density 2012	-0.84	0.71	GMSV/Satellite relationship
25	Satellite	NIR-1 2012	GMSV	Health 2016	0.84	0.70	-
26	Field	Health 2018	GMSV	Health 2016	0.83	0.69	Consistency over time
27	Satellite	NIR-2 2012	GMSV	Health 2016	0.83	0.69	-
28	Field	Health 2018	GMSV	Canopy Density 2016	0.83	0.69	-
29	Satellite	NIR-1 2012	GMSV	Canopy Density 2016	0.83	0.69	-
30	Field	Canopy Density 2018	GMSV	Canopy Density 2018	0.82	0.68	Field/GMSV relationship
31	Field	Canopy Density 2018	GMSV	Health 2018	0.82	0.67	Field/GMSV relationship
32	Field	Canopy Density 2018	GMSV	Canopy Density 2016	0.82	0.67	Consistency over time
33	Satellite	NIR-2 2012	GMSV	Canopy Density 2016	0.81	0.66	-
34	GMSV	Health 2016	GMSV	Canopy Density 2018	0.81	0.66	Consistency over time
35	GMSV	Canopy Density 2010	Satellite	NIR-1 2012	0.81	0.66	-
36	Satellite	NIR-1 2012	GMSV	Canopy Density 2012	0.81	0.66	GMSV/Satellite relationship
37	GMSV	Canopy Density 2010	Satellite	NIR-2 2012	0.81	0.65	-
38	Satellite	NIR-2 2012	GMSV	Canopy Density 2012	0.81	0.65	GMSV/Satellite relationship
39	Satellite	NIR-1 2010	GMSV	Canopy Density 2010	0.79	0.63	GMSV/Satellite relationship
40	Satellite	NIR-1 2010	GMSV	Canopy Density 2012	0.79	0.63	-
41	Field	Canopy Density 2018	GMSV	Health 2016	0.77	0.60	-
42	Satellite	Red Edge 2012	GMSV	Canopy Density 2016	-0.77	0.59	-
43	Satellite	NIR-1 2010	GMSV	Health 2010	0.77	0.59	GMSV/Satellite relationship
44	Satellite	NIR-1 2010	GMSV	Health 2012	0.77	0.59	-
45	GMSV	Health 2010	Satellite	Red Edge 2012	-0.76	0.57	-
46	Satellite	Red Edge 2012	GMSV	Health 2012	-0.76	0.57	GMSV/Satellite relationship
47	Satellite	NIR-1 2012	GMSV	Health 2018	0.74	0.55	-
48	GMSV	Health 2010	Satellite	NIR-1 2012	0.74	0.55	-
49	Satellite	NIR-1 2012	GMSV	Health 2012	0.74	0.55	GMSV/Satellite relationship
50	Satellite	Red Edge 2010	GMSV	Health 2016	-0.74	0.55	-
51	GMSV	Health 2010	Satellite	NIR-2 2012	0.74	0.55	-
52	Satellite	NIR-2 2012	GMSV	Health 2012	0.74	0.55	GMSV/Satellite relationship
53	GMSV	Health 2010	GMSV	Health 2016	0.74	0.54	Consistency over time
54	GMSV	Health 2012	GMSV	Health 2016	0.74	0.54	Consistency over time
55	GMSV	Canopy Density 2010	Satellite	Red 2012	0.74	0.54	-
56	Satellite	Red 2012	GMSV	Canopy Density 2012	0.74	0.54	GMSV/Satellite relationship
57	Satellite	NIR-2 2010	GMSV	Canopy Density 2010	0.74	0.54	GMSV/Satellite relationship
58	Satellite	NIR-2 2010	GMSV	Canopy Density 2012	0.74	0.54	-
59	Field	Health 2018	Satellite	Red 2018	-0.73	0.54	Field/satellite relationship
60	Field	SPAD Data average	Satellite	Red 2018	-0.73	0.53	SPAD/Satellite relationship
61	Satellite	NIR-2 2012	GMSV	Health 2018	0.73	0.53	-
62	Satellite	Red Edge 2012	GMSV	Health 2016	-0.72	0.52	-
63	Field	Height (feet)	Satellite	NIR-2 2012	0.72	0.51	Distance from sensor
64	Satellite	Red Edge 2016	Satellite	Red 2016	0.71	0.50	Satellite Self-consistency
65	Satellite	Red Edge 2010	GMSV	Canopy Density 2016	-0.71	0.50	
66	Satellite	NIR-2 2010	GMSV	Health 2010	0.70	0.49	GMSV/Satellite relationship
67	Satellite	NIR-2 2010	GMSV	Health 2012	0.70	0.49	-

Table 1. The highest ranked pairs of correlated variables from the study of *Ficus microcarpa* trees in Lakewood, California and the relevance of their relationship, if applicable, 2010 to 2018.

Trees with observed evidence of root pruning had an average health rating of 2.86, while those without evidence of root pruning have an average health rating of 3.73 ($p < 0.07$). Average canopy density was higher for trees without observed root pruning (64% density) than with observed root pruning (45% density) ($p < 0.08$).

When comparing the two sets of trees, there was no significant correlation between the SPAD values of the two sets of trees ($p < 0.43$), the Red-Edge reflectance data of the two sets ($p < 0.35$), and the Red reflectance of the two sets ($p < 0.25$). However, a significant difference was present between the Near Infrared-1 values for each group ($p < 0.06$) and the Near Infrared-2 values for each group ($p < 0.05$).

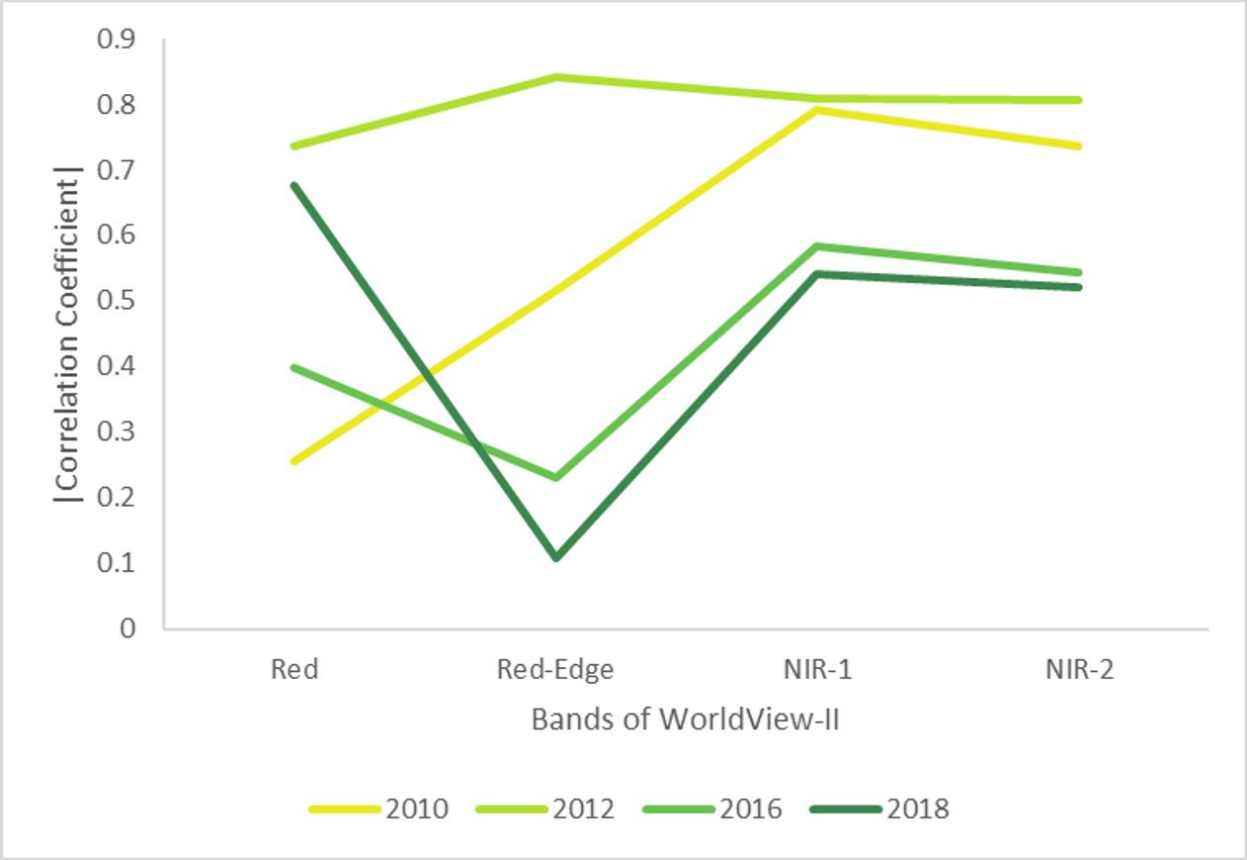

Fig. 4. The absolute values of correlation coefficients of canopy density assessed from GMSV and the pixel values of the Worldview-II satellite bands across all four years examined.

	Red	Red Edge	NIR-1	NIR-2	Canopy Density GMSV	Health GMSV	SPAD
Red	1.00	0.48	0.58	0.54	0.09	0.08	0.26
Red Edge		1.00	0.18	0.15	0.08	0.11	0.32
NIR-1			1.00	**0.98**	0.41	0.35	0.00
NIR-2				1.00	0.38	0.33	0.00
Canopy Density GMSV					1.00	**0.86**	0.01
Health GMSV						1.00	0.02
SPAD							1.00

Table 2. Correlation matrix showing r values for each of the variable pairs from the aggregated overall data, *Ficus microcarpa* trees in Lakewood, California, 2010 to 2018.

Discussion

We discerned five general categories of relevance to categorize each of the strong relationships recorded: (1) Field/GMSV Relationship, (2) GMSV/Satellite Relationship, (3) Consistency Over Time, (4) Observation Self-Consistency, and (5) Satellite Self-Consistency. The most significant relationships were those between the data collection phases of this research. A significant difference was present in the Near Infrared-1 and Near Infrared-2 values between groups of trees with and without an observed history of recent root cutting.

GMSV/Satellite Relationship

Two of the strongly correlating pairs of variables related the GMSV canopy density and health ratings to the Worldview-II Red-Edge reflectance data. The 2012 Red-Edge band had a strongly negative correlation with both 2012 canopy density ratings ($r \sim -0.84$) and health ratings ($r \sim -0.75$). The correlation between health and Red-Edge reflectance suggests the ability to use Red-Edge satellite data to predict tree health. This correlation infers that trees with lower Red-Edge reflectance are associated with healthier rankings in visual observations.

For the 2010 and 2012 data, the range of correlations across satellite bands and GMSV Canopy Density ratings were generally higher than in 2016 and 2018 (**Fig. 4**). Reflectance values from Near Infrared-1 and Near Infrared-2 correlated with each other ($r \sim 0.98$), and the canopy density ratings correlated with health ratings ($r \sim 0.84$), but a less-significant correlation existed between the GMSV ratings and the spectral reflectance data when the data were aggregated together over all four time periods of the study (**Table 2**).

One explanation for the 2010/2012 vs. 2016/2018 difference in correlation is the time of year difference between the satellite data and the available GMSV imagery. GMSV images from 2010/2012 were taken in March and April, the 2016 GMSV images were taken in April and May,

and the 2018 GMSV images were taken between January and April. Although *Ficus microcarpa* is an evergreen species, its color and reflectance change throughout the year. The Worldview-II spectral imagery was collected in the month of April for 2010, 2012, and 2018, and in the month of May for 2016. The mismatch of the time of year between the spectral data and the GMSV data (late May spectral paired with March/April GMSV in 2016 and April spectral paired with Jan/Feb GMSV in 2018) could be the reason for the much lower correlation in the latter two study years. This explanation is plausible because the 2010/2012 data are from similar times of year, albeit separated by one full year. During the 2010/2012 period, the GMSV was collected in March and April of 2011.

The 2010/2012 data was not more precise than the 2016/2018 data. Rather, image resolution and quality improved over the eight-year study period. It is possible the observed discrepancy between 2010/2012 correlations and 2016/2018 correlations indicates that the correlation observed in the 2010 and 2012 data is spurious, resulting from a relatively small number of data points (n=25 for each period).

SPAD/Satellite Relationship

The SPAD data did not significantly correlate with the Near Infrared-1 or Near Infrared-2 band values for 2018. The NIR light transmission of 940 nm used by the SPAD meter for chlorophyll assessments is within the Worldview-II Near Infrared-2 band (895 nm to 950 nm) (Uddling et al. 2007). An unknown confounding variable might have caused a difference between the infrared light transmitted to the SPAD meter and the infrared light that reached the satellite. It is possible that some of the leaves sampled with the SPAD meter had NIR transmittance values that were not representative of the majority of leaves within the tree, causing the chlorophyll values of the leaves not to correlate with the pixel values from the satellite.

In the Red band, the SPAD measurements did correlate with the values for 2018 ($r \sim -0.73$). The SPAD meter measures the Red transmittance of light at 650 nm in its chlorophyll measurements, which is within the Worldview-II Red reflectance range of 630-690 nm (Uddling 2007). It is possible the interference between satellites and our field measurement only affected the NIR wavelengths. Further research could test correlations for street trees between SPAD measurements and spectral reflectance captured by drones as well as satellites to see if an intermediate observation system is more highly correlated.

Root Pruning

A significant difference existed between the health and canopy density ratings for the group of trees that had evidence of root pruning and the group that did not ($p < 0.07$ and $p < 0.08$). Also, the differences between Near Infrared-1 and Near Infrared-2 reflectance were significant between the two groups of trees ($p < 0.06$ and $p < 0.05$). However, the differences among SPAD readings, Red reflectance, and Red-Edge reflectance were not significant ($p < 0.42$, $p < 0.35$, and $p < 0.25$). Near-Infrared bands measure a different physiological response than a reduction in chlorophyll content of leaves in the affected trees, the high reflectance is primarily due to the internal scattering within the leaf from cell structure. Unfortunately, our research is unable to provide a further explanation for this significant difference.

Field/GMSV Relationship

A strong correlation was present between the health and canopy density ratings recorded in the field and those recorded based on the GMSV data ($r > 0.82$). The correlation between field and GMSV health ratings from January-April 2018 had the strongest correlation ($r \sim 0.91$). The field ratings had stronger correlations to the 2018 GMSV data than other years' GMSV data because the condition of the trees changed over time, and the 2018 GMSV imagery was closest in time to the field observations. The relationship between field ratings and GMSV ratings shows consistency between the researchers' subjective assessments of the health and canopy density ratings.

Satellite Self-Consistency

Adjacent bands of reflected light collected at the same time had the strongest correlations. This pattern was seen at both the segmented level and the aggregated level. The strong correlation between adjacent reflectance bands demonstrated self-consistency. Because each band reflected the average value of reflected light within a given band, it might be expected that wavelengths near the division lines between bands could influence bands on either side of the line they straddle. This fact is an expected consequence of choosing defined bands for measurement on a continuous spectrum: wherever a dividing line is set, wavelengths will be on either side of it.

Consistency Over Time

Six sets of GMSV health and canopy density ratings had strong correlations between different years, showing consistency among the study trees over time. The curb replacement occurred at

the same place and time for Trees 1 through 44 and did not occur for Trees 45 through 51, inferring that without any externalities like pruning, the trees tended to correlate in how their condition rating changed over time. Observed deviations from inter-period correlation might have been related to the amount of root pruning that resulted from the curb replacement. No other differences in externalities were observed on-site or in the historical GMSV images.

Observation Self-Consistency

Within each given set of GMSV condition rating assessments in 2010, 2012, 2016, and 2018 the canopy density and health ratings had high correlations ($r > 0.88$). Authors Komen and Hodel subjectively rated both variables for all trees in each of the study periods. These variables likely correlate strongly because canopy density is an empirical attribute that is used to determine the health rating of a tree when making visual assessments. A tree with a sparser canopy tends to be assigned a lower health rating, and a tree with a denser canopy tends to be assigned a higher health rating. Differences between canopy density and health can be accounted for by trees that had significantly died back in the past but were vigorously resprouting at the time of observation; their overall canopy densities were low at the time of observation, but their health ratings had increased because the growth that was present was healthy.

Conclusions

Strong correlations existed between health and canopy density measurements in the field and canopy density and health measurements from GMSV, which indicates a potential to use GMSV imagery to update visual tree health rankings in city inventories in lieu of sending arborists into the field. GMSV health ratings were strongly negatively correlated with Red-Edge reflectance data from the Worldview-II satellite, indicating a potential to use satellite reflectance values to observe declining health conditions for individual street trees. This result was inconsistent across all four years in this study, which could be due to changes in the resolution and quality of the Worldview-II satellite between 2012 and 2016, atmospheric interference or other unknown variables. Satellite reflectance values in the NIR can capture change in tree health that are not visible to the naked eye and may be considered in assessments of tree health to predict tree health decline. Future research should include a larger sample size of trees and additional years of satellite imagery to determine if the negative correlation between GMSV ratings and Red-Edge reflectance data can be replicated across broader scales and at other study sites. At the conclusion of this study, all trees were removed due to bad health. Future studies could include trees that are in good health to test if the correlations observed in this study apply to trees in good health. Other topics of future research could include exploring the relationship between a

history of root cutting and satellite spectral measurements of urban street trees to determine if negative health effects from root cutting can be observed via satellite.

Acknowledgements

The authors are grateful for the support of the City of Lakewood and their staff for collaboration on the field data collection phase: Grant Pickering, Tim Hunt, Tyler Bautista, Marc McMurray, Rick Kapella, and Andrew Schade. Donald J. Merhaut, University of California, Riverside, provided the SPAD meter. We are grateful to K. N. Au and Geocarto International Centre Limited for the spectral reflectance analysis of the 25 trees using WorldView-2 satellite data.

Literature Cited

Carreiro, M. M., Y. C. Song, and J. Wu (Eds.). 2007. Ecology, Planning, and Management of Urban Forests: International Perspective. Springer New York, Germany.

Cumming, A. B., D. B. Twardus, and D. J. Nowak. 2008. Urban forest health monitoring: large-scale assessments in the United States. Arboriculture & Urban Forestry 34 (6): 341–346. https://doi.org/10.48044/jauf.2008.047

Fang, F., B McNeil, T. Warner, G. Dahle, and E. Eutsler. 2020. Street tree health from space? An evaluation using WorldView-3 data and the Washington DC Street Tree Spatial Database. Urban Forestry & Urban Greening 49: 126634. https://doi.org/10.1016/j.ufug.2020.126634

Hodel, D. R., A. J. Downer, and D. M. Mathews. 2009. Sooty canker, a devastating disease of Indian laurel-leaf fig trees. West. Arb. 35(4): 28–32.

Horler, D. N. H., M. Dockray, and J. Barber, J. 1983. The red edge of plant leaf reflectance. International Journal of Remote Sensing 4(2): 273–288. https://doi.org/10.1080/01431168308948546

Knipling, E. B. 1970. Physical and physiological basis for the reflectance of visible and near-infrared radiation from vegetation. Remote Sensing of Environment 1(3): 155–-159. https://doi.org/10.1016/S0034-4257(70)80021-9

Livesley, S. J., E. G. McPherson, and C. Calfapietra. 2016. The urban forest and ecosystem services: impact on urban water, heat, and pollution cycles at the tree, street, and city scale. Journal of Environmental Quality. 45: 119–124. https://doi.org/10.2134/jeq2015.11.0567

Malthus, T. J., C. J. Younger, H. Birchwoods, and M. Littleburn. 2000. Remotely sensing stress in street trees using high spatial resolution data, Vol. 2, pp. 326–333 *in*: Proceedings of the 2nd International Geospatial Information in Agriculture and Forestry Conference, 10–12 January 2000, Lake Buena Vista, Florida, U.S.A.

Mayorquin, J. S., A. J. Downer, D. R. Hodel, A. Liu, and A. Eskalen. 2012**a**. *Ficus* branch canker of Indian laurel-leaf fig. West. Arb. 38(1): 60–61.

Mayorquin, J. S., A. Eskalen, A. J. Downer, D. R. Hodel, and A. Liu, A. 2012**b**. First report of multiple species of the Botryosphaeriaceae causing bot canker disease of Indian laurel-leaf fig in California. Plant Disease 96(3): 459–459. https://doi.org/10.1094/PDIS-08-11-0714

McPherson, E. G., N. van Doorn, and J. de Goede. 2016. Structure, function and value of street trees in California, USA. Urban Forestry & Urban Greening 17: 104–115. https://doi.org/10.1016/j.ufug.2016.03.013

Morgenroth, J. and J. Östberg. 2017. Measuring and monitoring urban trees and urban forests, pp. 33–48 *in*: Routledge Handbook of Urban F. Routledge.

Richards, D. R., and P. J. Edwards. 2017. Quantifying street tree regulating ecosystem services using Google Street View. Ecological Indicators 77: 31–40. https://doi.org/10.1016/j.ecolind.2017.01.028

Robson, A. J., J. Petty, D. C. Joyce, J. R. Marques, and P. J Hofman. 2014. High resolution remote sensing, GIS and Google Earth for avocado fruit quality mapping and tree number auditing, pp. 589–596, in: XXIX International Horticultural Congress on Horticulture: Sustaining Lives, Livelihoods and Landscapes (IHC2014): 1130. https://10.17660/ActaHortic.2016.1130.88

Uddling, J., J. Gelang-Alfredsson, K. Piikki, and H. Pleijel. 2007. Evaluating the relationship between leaf chlorophyll concentration and SPAD-502 chlorophyll meter readings. Photosynthesis Research 91(1): 37–46. https://doi.org/10.1007/s11120-006-9077-5

US Census Bureau Public Information Office. Growth in Urban Population Outpaces Rest of Nation. United States Census Bureau Newsroom, 2010 Census, 19 May 2016, https://www.census.gov/newsroom/releases/archives/2010_census/cb12-50.html

Wu, S., X. Ding, R. Liu, and H. Gao. (2019). How does IT capability affect open innovation performance? The mediating effect of absorptive capacity. European Journal of Innovation Management 24: 43-65. 10.1108/EJIM-02-2019-0043

Wu, J., D. Wang, C. J. Rosen, and M. E. Bauer. 2007. Comparison of petiole nitrate concentrations, SPAD chlorophyll readings, and QuickBird satellite imagery in detecting nitrogen status of potato canopies. Field Crops Research 101(1): 96–103. https://doi.org/10.1016/j.fcr.2006.09.01

Xia, Y., N. Yabuki, and T. Fukuda. 2021. Development of a system for assessing the quality of urban street-level greenery using street view images and deep learning. Urban Forestry & Urban Greening 59: 126995. https://doi.org/10.1016/j.ufug.2021.126995

Xie, Q., J. Dash, W. Huang, D. Peng, Q. Qin, H. Mortimer, R. Casa, S. Pignatti, G. Laneve, S. Pascucci, Y. Dong, and H. Ye. 2018. Vegetation indices combining the red and red-edge spectral information for leaf area index retrieval. IEEE Journal of Selected Topics in Applied Earth Observations and Remote Sensing 11(5): 1482–1493. doi: 10.1109/JSTARS.2018.2813281

Xie, Y., Z. Sha, and M. Yu. 2008. Remote sensing imagery in vegetation mapping: a review. Journal of Plant Ecology 1(1): 9–23. https://doi.org/10.1093/jpe/rtm005

James Komen is a consulting arborist in California specializing in risk assessment and tree appraisal. *jameskomen@gmail.com*

Camille C. Pawlak is a graduate student at the University of California, Los Angeles studying urban trees. camipawlak@ucla.edu

Donald R. Hodel is emeritus landscape horticulture advisor for the University of California Cooperative Extension in Los Angeles. *drhodel@ucanr.edu*

Publication Date: 2 September 2023.

PalmArbor: *http://ucanr.edu/sites/HodelPalmsTrees/PalmArbor/*
ISSN 2690-3245
Editor-In-Chief: Donald R. Hodel
Hodel Palms and Trees: *http://ucanr.edu/sites/HodelPalmsTrees/*